ELSEVIER

Neurobiology of Aging 30 (2009) 2021–2030

NEUROBIOLOGY OF AGING

www.elsevier.com/locate/neuaging

IGF-1 signaling reduces neuro-inflammatory response and sensitivity of neurons to MPTP

Agnès Nadjar[a,1], Olivier Berton[b], Shuhong Guo[c], Patricia Leneuve[d], Sandra Dovero[a], Elsa Diguet[a], François Tison[a], Baolu Zhao[c], Martin Holzenberger[d], Erwan Bezard[a,*]

[a] *Université Victor Segalen Bordeaux 2, Centre National de la Recherche Scientifique, Bordeaux Institute of Neuroscience, UMR 5227, Bordeaux, France*

[b] *Department of Psychiatry, University of Pennsylvania Medical School, Philadelphia, PA, USA*

[c] *State Key Laboratory of Brain and Cognitive Science, Institute of Biophysics, Chinese Academy of Sciences, Beijing, China*

[d] *INSERM U515, Hôpital Saint-Antoine, Paris, France*

Received 14 December 2007; received in revised form 9 February 2008; accepted 20 February 2008
Available online 3 April 2008

Abstract

Reduced expression of IGF-1R increases lifespan and resistance to oxidative stress in the mouse, raising the possibility that this also confers relative protection against the pro-parkinsonian neurotoxin MPTP, known to involve an oxidative stress component. We used heterozygous IGF-1R$^{+/-}$ mice and challenged them with MPTP. Interestingly, MPTP induced more severe lesions of dopaminergic neurons of the substantia nigra, in IGF-1R$^{+/-}$ mice than in wild-type animals. Using electron spin resonance, we found that free radicals were decreased in IGF-1R$^{+/-}$ mice in comparison with controls, both before and after MPTP exposure, suggesting that the increased vulnerability of dopamine neurons is not caused by oxidative stress. Importantly, we showed that IGF-1R$^{+/-}$ mice display a dramatically increased neuro-inflammatory response to MPTP that may ground the observed increase in neuronal death. Microarray analysis revealed that oxidative stress-associated genes, but also several anti-inflammatory signaling pathways were downregulated under control conditions in IGF-1R$^{+/-}$ mice compared to WT. Collectively, these data indicate that IGF signaling can reduce neuro-inflammation dependent sensitivity of neurons to MPTP.

Keywords: Insulin-like growth factor; Neurodegeneration; Oxidative stress; Neuro-inflammation; Microglia

1. Introduction

Insulin-like growth factor-1 (IGF-1) is a multifunctional peptide essential for normal growth and development (Russo et al., 2005) whose pleiotropic actions are mediated primarily by insulin-like growth factor type 1 receptor (IGF-1R), a transmembrane, ligand-activated tyrosine kinase highly homologous to the insulin receptor. Partial inactivation of the IGF-1R increases lifespan and resistance to oxidative stress in the mouse (Holzenberger et al., 2003). Important reciprocal interactions have also been demonstrated between IGF-1 and the pro-inflammatory cytokines that mediate neuro-inflammation (Venters et al., 1999; Ye et al., 2003; Kenchappa et al., 2004). Recent research revealed an anti-inflammatory action, counteracting pro-inflammatory effects of cytokine tumor necrosis factor alpha (TNF-α) (Bluthe et al., 2006). According to the context, IGF-1 would thus appear capable of antagonistic action, pro-oxidative or anti-inflammatory.

1-Methyl-4-phenyl-1,2,3,6-tetrahydropyridine (MPTP), used for modelling the selective dopaminergic cell injury

* Corresponding author at: CNRS UMR 5227, Université Victor Segalen, 146 rue Léo Saignat, 33076 Bordeaux Cedex, France.
Tel.: +33 5 57 57 16 87; fax: +33 5 56 90 14 21.
E-mail addresses: agnes.nadjar@u-bordeaux2.fr (A. Nadjar), bertonol@mail.med.upenn.edu (O. Berton), hbgsh@moon.ibp.ac.cn (S. Guo), patricia.leneuve@st-antoine.inserm.fr (P. Leneuve), sandra.dovero@u-bordeaux2.fr (S. Dovero), elsa.diguet@cea.fr (E. Diguet), Francois.Tison@chu-bordeaux.fr (F. Tison), zhaobl@sun5.ibp.ac.cn (B. Zhao), Martin.Holzenberger@st-antoine.inserm.fr (M. Holzenberger), erwan.bezard@u-bordeaux2.fr (E. Bezard).
[1] Present address: CNRS UMR 5226, INRA UMR1286, Université Bordeaux 2, Bordeaux, France.

0197-4580/$ – see front matter © 2008 Elsevier Inc. All rights reserved.
doi:10.1016/j.neurobiolaging.2008.02.009

occurring in Parkinson's disease, has dual inflammatory and oxidative actions, but these are non-antagonistic. 1-Methyl-4-phenyl pyridinium (MPP+), the active metabolite of MPTP induces the formation of reactive oxygen species (ROS), such as superoxide or hydroxyl radicals (Blum et al., 2001; Wang et al., 2001; Ryu et al., 2003; Tunez et al., 2004; Watanabe et al., 2005), suggesting that one of the causes of the neurotoxic action is oxidative stress. MPTP concomitantly activates neuro-inflammatory processes, of which the most important are reactive astrogliosis and microgliosis (Reinhard et al., 1988; Francis et al., 1995; Brouillet et al., 1999; Kurkowska-Jastrzebska et al., 1999) and cytokine synthesis (Rousselet et al., 2002; Hebert et al., 2003; Pera et al., 2004; Pattarini et al., 2007). Finally, during MPTP intoxication in mice, IGF-1R levels are upregulated but AKT phosphorylation remained unchanged (D'Astous et al., 2006), showing that while IGF signalling pathways are active in the brain under this neurotoxic insult, IGF signalling activity is not necessarily further induced by this stress.

To better understand the cellular mechanism underlying the antagonistic pro-oxidant and anti-inflammatory action of IGF-1, we submitted heterozygous IGF-1R$^{+/-}$ mice to acute MPTP intoxication. The lesions induced by MPTP were more severe in these mice than in wild-type control animals. The IGF-1R$^{+/-}$ group also showed lower levels of both nitric oxide (NO) and reactive oxygen species (ROS) than controls, both before and after MPTP treatment, but displayed, on the other hand, a dramatically increased neuro-inflammatory response that could well explain the observed increase in neuronal death.

2. Experimental procedure

2.1. Animals

We established a targeted IGF-1R gene knockout on 129/Sv genetic background (Holzenberger et al., 2003) and backcrossed the mutants for >15 generations to C57BL/6 mice. IGF-1 receptor levels in IGF-1R$^{+/-}$ mice were half those in WT (IGF-1R$^{+/+}$) mice. Homozygous IGF-1R$^{-/-}$ knockout mutants invariably die minutes after birth. For this study we used 40 IGF-1R$^{+/-}$ and 38 WT (IGF-1R$^{+/+}$) littermates, as controls. All mice were males and were used at similar age (10–12 weeks) in the different experiments. They were maintained under SPF conditions in individually ventilated filter cages at 23 ± 1 °C, with a 14/10-h light/dark cycle and free access to water and a commercial rodent diet. Body weight was measured before i.p. injections and at the time of sacrifice. Experiments were conducted according to institutional guidelines and European Communities Council Directive 86/609/EEC for the care of laboratory animals. Every effort was made to minimize animal suffering and to use only the minimum number of individuals necessary to perform statistically valid analysis.

2.2. MPTP intoxication and measurement of MPP+ levels

Mice were submitted to acute MPTP challenge consisting of two intraperitoneal (i.p.) injections of 30 mg/kg body weight at 3 h interval (9:00 a.m. and 12:00 a.m.). Time lapse between the final injection of MPTP and sacrifice varied according to the subsequent analysis. For TH immuohistochemical analysis, mice that were killed 7 days after MPTP intoxication, i.e. a time interval of 7 days that must be respected after MPTP exposure and before sacrifice for the assessment of nigral degeneration by TH-IR neuronal count (phenotypical marker) in the mouse midbrain (Jackson-Lewis et al., 1995).

As a drug could protect from MPTP by interfering with MPTP metabolism, we checked the MPP+ levels as previously described (Bezard et al., 2003). Eight mice (four IGF-1R$^{+/-}$ and four WT) received one dose of MPTP (30 mg/kg i.p.) and were killed 120 min after MPTP injection. Brains were rapidly removed and the caudate–putamen complex dissected out on ice. Tissue samples were sonicated in 10 volumes of 5% trichloroacetic acid containing 20 mg/ml 4-phenylpyridine (Sigma–Aldrich, Saint Quentin Fallavier, France) as internal standard. Homogenates were centrifuged at 15,000 × *g* for 20 min at 4 °C and the contents of MPP+ in the resulting supernatants were quantified by HPLC with UV detection. MPP+ was monitored at 295 nm and flow rate was set at 1.5 ml/min. Quantification was made by comparison of peak height ratios in the samples with those of the standards.

2.3. Immunohistochemistry

2.3.1. Tissue processing

After MPTP administration, mice were anesthetized with urethane, then perfused with 0.9% NaCl followed by 4% paraformaldehyde (PFA). Brains were removed, postfixed in 4% PFA for 2 days at 4 °C, immersed in 20% sucrose, frozen by slow immersion in isopentane cooled on dry ice to −45 °C, and stored at −80 °C. We used a cryostat at −17 °C to cut 25 μm coronal sections, which were collected free floating for immunohistochemistry.

2.3.2. TH immunohistochemistry

TH immunohistochemistry was performed 7 days after MPTP injections (Jackson-Lewis et al., 1995). Serum containing TH antibody (polyclonal rabbit TH antibody, J. Boy, Reims, France) was diluted 1:2000 in phosphate-buffered saline (PBS) containing 0.3% Triton X-100 and 1% bovine serum albumin (BSA), and sections were incubated overnight at 4 °C, before being incubated for 2 h with biotinylated horse anti-rabbit antibody (universal secondary antibody, AbCys SA, Paris, France) diluted 1:500 in PBS/1% BSA/0.3% Triton X-100, for 2 h with avidin–biotin peroxidase diluted 1:200 in PBS (Vectastain ABC kit; Vector Laboratories, Burlingame, CA), and finally revealed with 3,3′-diaminobenzidine tetrahydrochloride (DAB kit, Vector

Laboratories). Sections were then slide-mounted and counterstained with cresyl violet.

2.3.3. CD11b immunohistochemistry

CD11b immunohistochemistry was performed 24 h after MPTP injections. After 30 min in blocking buffer (PBS/0.3% horse serum (HS)/0.3% H_2O_2), sections were incubated with rat anti-mouse CD11b antibody (Serotec, Raleigh, NC) diluted 1:500 in PBS/2% HS overnight at 4 °C, before being incubated for 90 min in biotinylated anti-rat antibody (1:500 in PBS) (Amersham Biosciences, Buckinghamshire, UK). Sections were then processed as for TH immunoreactivity (ABC kit, 1:1000, 90 min and DAB kit, counterstaining with cresyl violet).

2.3.4. Stereology and counting of tyrosine hydroxylase immunoreactive (ir) neurons

For counting TH-ir neurons (phenotypic marker) and Nissl stained cells (structural marker) in the SNc, we used the unbiased stereological sampling method (Gundersen et al., 1988; West and Gundersen, 1990) based on optical dissector stereological probe, as previously described (Bezard et al., 2003; Gross et al., 2003). Stereological analysis was performed using an Leica DMRE microscope with a motorized Z and X-Y stage encoders linked to a computer-assisted stereological system (Mercator Digital Imaging System, Explora Nova, La rochelle, France). For each animal, SNc boundaries were delimited at low magnification (2.5×) by examining the size and shape of the different groups of TH-ir neurons and their axonal projections, as well as nearby fiber bundles according to Franklin & Paxinos mouse brain atlas. SNc boundaries are drawn on every sixth section and the first was randomly chosen. SNc volume was calculated using the formula $V_{(SNc)} = \Sigma S\, td$; where ΣS is the sum of surface areas (μm^2), t the average section thickness (and d the distance between the sections (Theoret et al., 1999)). The average section thickness (t) was estimated to 12 μm after immunohistochemistry processing and guard zones of 2 μm were used to ensure that top and bottom of sections are never included in the analysis. Eleven sections were used for each animal. From a random start position, a computer-generated sampling grid placed the counting frames. The counting frame size was length 50 μm and width 40 μm. We left a distance of 30 μm (x) and 20 μm (y) between each counting frame. Within each frame, all cell nuclei were counted which came into focus (40× immersion oil objective) (Gundersen et al., 1988). A neuron was counted if more than half the cell body was inside the two consecutive boundaries taken into account. To estimate the number of TH-ir neurons we used: $N = V_{(SNc)}\ (\Sigma Q^- / \Sigma V_{(dis)})$; where N is the estimation of the number of TH-ir neurons, V the volume of the SNc, ΣQ^- the number of cells counted in the frames, and $\Sigma V_{(dis)}$ is the total volume of the frames (Theoret et al., 1999). Mean estimated number of neurons and SEM were then calculated for each group (WT or +/−/NaCl; WT or +/−/MPTP).

2.3.5. Quantification of TH-ir striatal density

Striatal TH-ir density was assessed in the dorsolateral striatum by densitometric analysis of sections using an image analysis system (Biocom, Visioscan v4.12, Les Ulis, France) as previously described (Bezard et al., 2000; Guigoni et al., 2005). Three sections per animal were analyzed by an examiner blind with regard to the experimental condition. Optical densities were averaged in each animal and expressed as a percentage of control values obtained from saline-treated WT animals.

2.3.6. Quantification of CD11b-ir cells

Brain sections were examined under light microscopy using an image analysis system (Mercator; Explora Nova, La Rochelle, France). Four sections per animal were analyzed by an examiner blind to experimental conditions. Structures considered were the striatum and the SNc. An optical dissector probe was used to count the cells per mm^2 for each brain region per animal at a 40× magnification. Where CD11b immunoreactivity was present only in cellular ramifications, cells were not considered as positive microglia. Microglia was counted in the whole slice thickness, only if more than half the cell was inside the two consecutive boundaries taken into account. Split cell counting error was corrected by using the Abercrombie formula (Abercrombie, 1946). Mean cell number per plane and SEM were then calculated for each group of mice.

2.4. ROS and NO detection

To detect ROS and NO levels in the substantia nigra (encompassing both the pars compacta and reticulata, striatum and hippocamus we used a previously published method with minor modifications (Cao et al., 2005)). Mice were sacrificed 2 h after the last MPTP injection and both hemispheres weighed. Hand-dissected structures were homogenized in 1 ml of a spin trap solution containing 100 mM *N-tert*-butyl-α-phenylnitrone (PBN) and 2 mM diethyldithiocarbamate (DETA), to which we added 10 mM HEPES in ice-cold phosphate-buffered saline (PBS), followed by 0.5 M Na_2SO_4, 10 mM arginine, 0.3 M $FeSO_4$, 10 mM $CaCl_2$, before vortexing for 30 min. We then added 500 μl of ethyl acetate, vortexed for 30 s and centrifuged at 10,000 × g for 5 min. The ethyl acetate phase was transferred to a quartz cell for ESR study at room temperature. To quantify the intensity of the ROS signal, we measured the height of the second peak from the ESR spectra of PBN spin adducts ($g = 2.005$). For the NO signal, we measured and combined the height of the three peaks ($g = 2.035$). This approach proved more accurate than methods previously described (Shen et al., 2000). We used the following Bruker ER-200 X-band ESR spectrometer settings for trapping the free radicals: center field, 3445 G; scan width 200 G (usual setting for ROS and NO detection: 400 G); microwave frequency 9.47 GHz; modulation frequency 100 kHz; microwave power 20 mW; modulation amplitude 1 G (usual setting for ROS and NO detection 3.2 G).

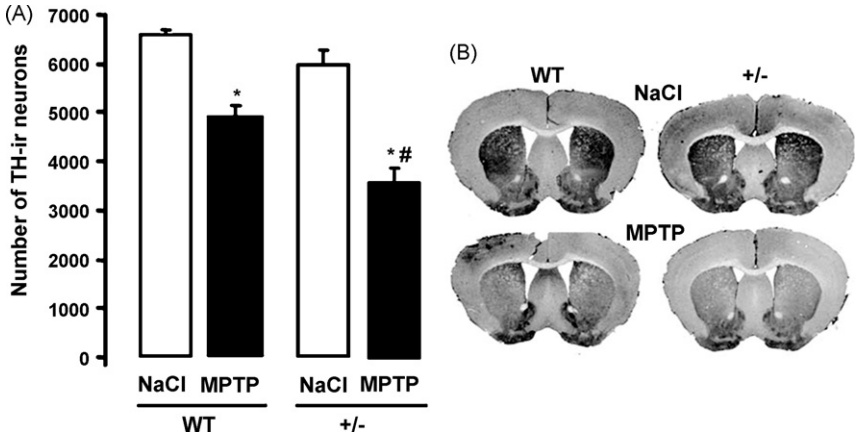

Fig. 1. MPTP treatment increases SNc lesions in IGF-1R$^{+/-}$ mice compared to WT. (A) Stereological counting of TH-ir neurons in the SNc of MPTP vs. NaCl-treated mice (*$P < 0.001$ vs. respective NaCl; $^{\#}P < 0.01$ vs. WT/MPTP; $n = 6$ for WT/NaCl, WT/MPTP, +/−/NaCl; $n = 9$ for +/−/MPTP). (B) Representative examples of TH immunostaining in the striatum of MPTP vs. NaCl-treated mice.

2.5. Microarray analysis

A total of $n = 9$ WT and $n = 9$ IGF-1R$^{+/-}$ mice were used for analysis of patterns of gene expression in the striatum using microarrays according to previously described procedures (Berton et al., 2006). Striatal tissue dissected from three mice was pooled and RNA extracted using TriZol reagent (Invitrogen, Carlsbad, CA) followed by a purification step using RNEasy columns (Qiagen, Valencia, CA). All RNA used for the study showed 260/280 nm ratio greater than 1.80, and RIN values from Agilent 2100 bioanalyzer greater than 8.0. Total RNA (2.5 μg) from each pooled sample was used for cDNA synthesis, cleanup, and labeling. We utilized the following kits and instructions from Affymetrix: GeneChip Expression 3′ Amplification OneCycle cDNA synthesis Kit (#900431), Affymetrix GeneChip Sample Cleanup Module (#900371), and Affymetrix IVT labeling kit (#900449). cRNA was only used if the total RNA recovered after amplification was >30 μg and 260/280 nm ratio greater than 1.90. From each sample, 20 μg of cRNA was fragmented and subsequently hybridized to GeneChip® Mouse Genome 430 2.0 Array (Affymetrix) by the UT Southwestern microarray core using standard procedures. Three independent arrays, derived from independent tissue samples, were analyzed for each experimental group. Raw data were analyzed initially using Microarray Suite version 5.0 (MAS 5.0, Affymetrix), which was used for quality control analysis, to scale all values to a target value (250), and to generate a list of 'absent' genes. Arrays were judged as acceptable for additional analysis if the 3′/5′ ratio of GAPDH and β-actin was less than 3, and the percentage of genes found to be 'present' was similar from array to array. This data file was imported into Arrayassist (Stratagene, La Jolla, CA) for GCRMA (GC Robust Multi-array Average) background adjustment, quantile normalization, and median-polish summarization of all scaled values. Next, data files were imported into Genespring (Agilent) for final analysis and data visualization. Using the MAS 5.0 generated gene list of 'present' and 'absent' calls, genes were only analyzed if found to have a statistically significant signal in at least one of the experimental conditions (reducing gene list from approximately 30,000 genes to approximately 19,000 genes). Based on recommendations from the Microarray Quality Control Comparison project (MAQC-Consortium, 2006), we generated our differentially expressed gene lists using fold change primary criteria with a non-stringent *P*-value cutoff. Each differentially expressed gene list was generated by creating a volcano plot comparing each IGF-1R$^{+/-}$ genotype to the control condition (WT). We selected genes >1.3-fold differentially expressed with a $P < 0.05$, using a parametric *t*-test corrected for multiple comparisons. Pathway analyses were performed using the Ingenuity® software.

2.6. Statistical analysis

Data were presented as mean ± S.E.M. Two-way ANOVAs were used to estimate overall significance followed by *post hoc* Tukey's tests corrected for multiple comparisons unless specified otherwise. For MPP+ levels, a two-tailed unpaired *t*-test was used. For *post hoc* analysis of the microarray dataset the ingenuity© software relies on a right-tailed Fisher Exact Test to determine significant relative involvement of specific signalling pathways. A probability level of 5% ($P < 0.05$) was considered significant.

3. Results

3.1. IGF-1R$^{+/-}$ mice show increased loss of mesencephalic dopamine neurons after MPTP treatment

Holzenberger et al. (2003) showed that partial inactivation of IGF-1R increases lifespan and resistance to oxidative stress in the mouse, also raising the possibility that this confers relative protection against neurotoxins involving an oxidative stress response such as MPTP (complex

I inhibitor). Under control conditions, both IGF-1R$^{+/-}$ animals and their WT littermates showed similar estimated numbers of TH-ir neurons within the SNc (Fig. 1A). After MPTP treatment, WT mice had 26% less dopaminergic neurons in the SNc than under control conditions (two-way ANOVA; $P<0.001$), whereas IGF-1R$^{+/-}$ mice showed a 40% decrease of TH-ir neurons ($P<0.001$). The difference in the number of TH-ir neurons between MPTP-treated WT and IGF-1R$^{+/-}$ mice was statistically significant (two-way ANOVA; $F_{(3,26)}=11.9$; $P=0.002$) (Fig. 1A).

Striatal sections were immunostained for TH in the same four groups of mice. As can be seen from the example shown in Fig. 1B, both IGF-1R$^{+/-}$ animals (0.98 ± 0.4) and their WT littermates (1.0 ± 0.02) showed similar TH-ir in the striatum in control conditions. After MPTP treatment (two-way ANOVA; $F_{(3,26)}=40.05$; $P<0.0001$), WT mice had less TH-ir fibers in the striatum than under control conditions (two-way ANOVA; 0.68 ± 0.03; $P<0.001$), whereas IGF-1R$^{+/-}$ mice showed an even greater decrease (two-way ANOVA; 0.51 ± 0.05; $P<0.001$ vs. saline-treated IGF-1R$^{+/-}$ and $P<0.05$ vs. MPTP-treated WT) (Fig. 1B).

These compelling data indicate that IGF-1R$^{+/-}$ mice are more sensitive to MPTP treatment than WT mice.

3.2. MPP+ exposure is comparable in IGF-1R$^{+/-}$ and WT mice

Striatal MPP+ content was not different ($P=0.72$, two-tailed unpaired t test) in IGF-1R$^{+/-}$ (7.7 ± 0.7 μg/mg of tissue, $n=4$) and WT (8.1 ± 0.6 μg/mg of tissue, $n=4$) mice that received a single injection of 30 mg/kg MPTP (Bezard et al., 2003). Thus, the increased toxicity in IGF-1R$^{+/-}$ mice was not due to an increased delivery of MPTP to the brain following intraperitoneal injection, nor to increased brain biotransformation of MPTP to MPP+, or to increased striatal mitochondrial monoamine oxidase B activity.

3.3. Free radical release is lower in IGF-1R$^{+/-}$ than in WT mice after MPTP treatment

Holzenberger et al. (2003) demonstrated that IGF-1R$^{+/-}$ mice are less sensitive to paraquat-induced oxidative stress. To further substantiate their results, they induced oxidative damage in cultured mouse embryonic fibroblasts (MEFs) by low concentrations of H_2O_2 and found that the proportion of surviving cells was significantly higher in IGF-1R$^{+/-}$ than in control MEFs. However, considering the extended dopaminergic lesion observed in our experimental conditions in heterozygous knockout mice, we hypothesized that free radical production under MPTP would be higher in IGF-1R$^{+/-}$ mice than in WT, resulting in over-neurodegeneration. Using ESR, we thus evaluated NO and ROS content in three cerebral structures: the hippocampus (all regions of the hippocampus were studied), the substantia nigra (both compacta and reticulata) and the striatum (Fig. 2A and B). NO and ROS production was significantly higher in WT mice after MPTP

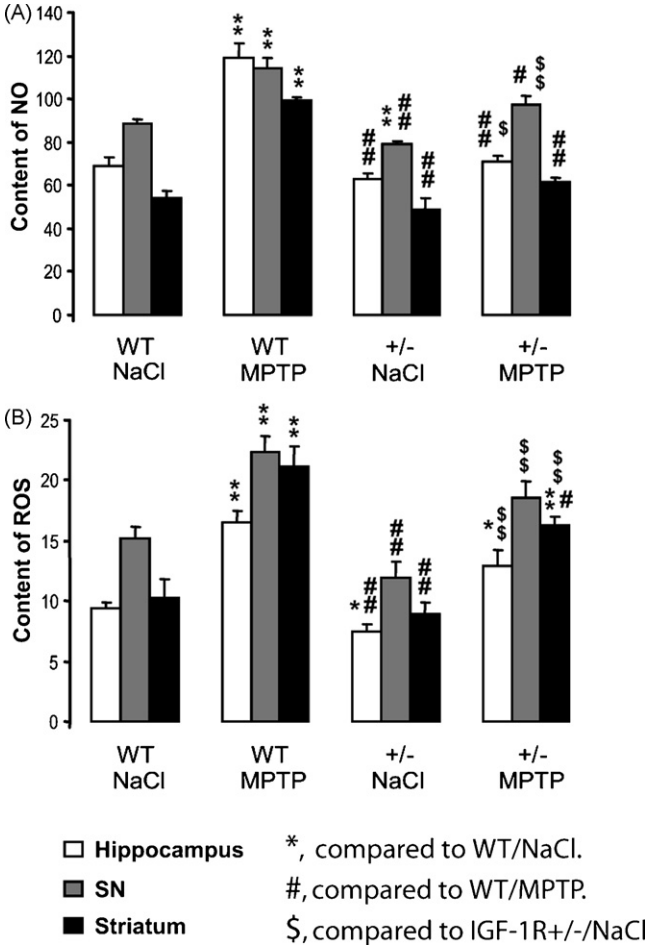

Fig. 2. MPTP-induced NO and ROS production is lower in IGF-1R$^{+/-}$ mice than in WT, in hippocampus, SN and striatum. (A) NO production in each structure, in WT and IGF-1R$^{+/-}$ mice, treated or not with MPTP (arbitrary unit/mg of protein). (B) ROS production in each structure, in WT and IGF-1R$^{+/-}$ mice, treated or not with MPTP (arbitrary unit/mg of protein) $^{*}P<0.05$; $^{**}P<0.01$ compared with WT/NaCl. $^{\#}P<0.05$; $^{\#\#}P<0.01$ compared with WT/MPTP. $^{\$}P<0.05$; $^{\$\$}P<0.01$ compared with IGF-1R$^{+/-}$/NaCl ($n=6$ for WT/NaCl, WT/MPTP, +/−/NaCl; $n=9$ for +/−/MPTP).

intoxication (two-way ANOVA; $P<0.01$, for each structure). In contrast, the increase of free radical production after MPTP treatment was much less pronounced in IGF-1R$^{+/-}$ mice (two-way ANOVA; $P<0.05$ or $P<0.01$, depending on the structure considered). Remarkably, we found that NO and ROS were decreased in IGF-1R$^{+/-}$ mice in comparison with controls, both before and after MPTP exposure, in SN, hippocampus and striatum (two-way ANOVA; $P<0.05$ or $P<0.01$). This suggested that the increased vulnerability of dopamine neurons is not caused by an increased exposure to cellular oxidative stress.

3.4. Neuro-inflammatory processes are enhanced in IGF-1R$^{+/-}$ mice after MPTP treatment

The neurotoxin MPTP is highly neuro-inflammatory inducing microglial activation (Hirsch et al., 2005; Nagatsu

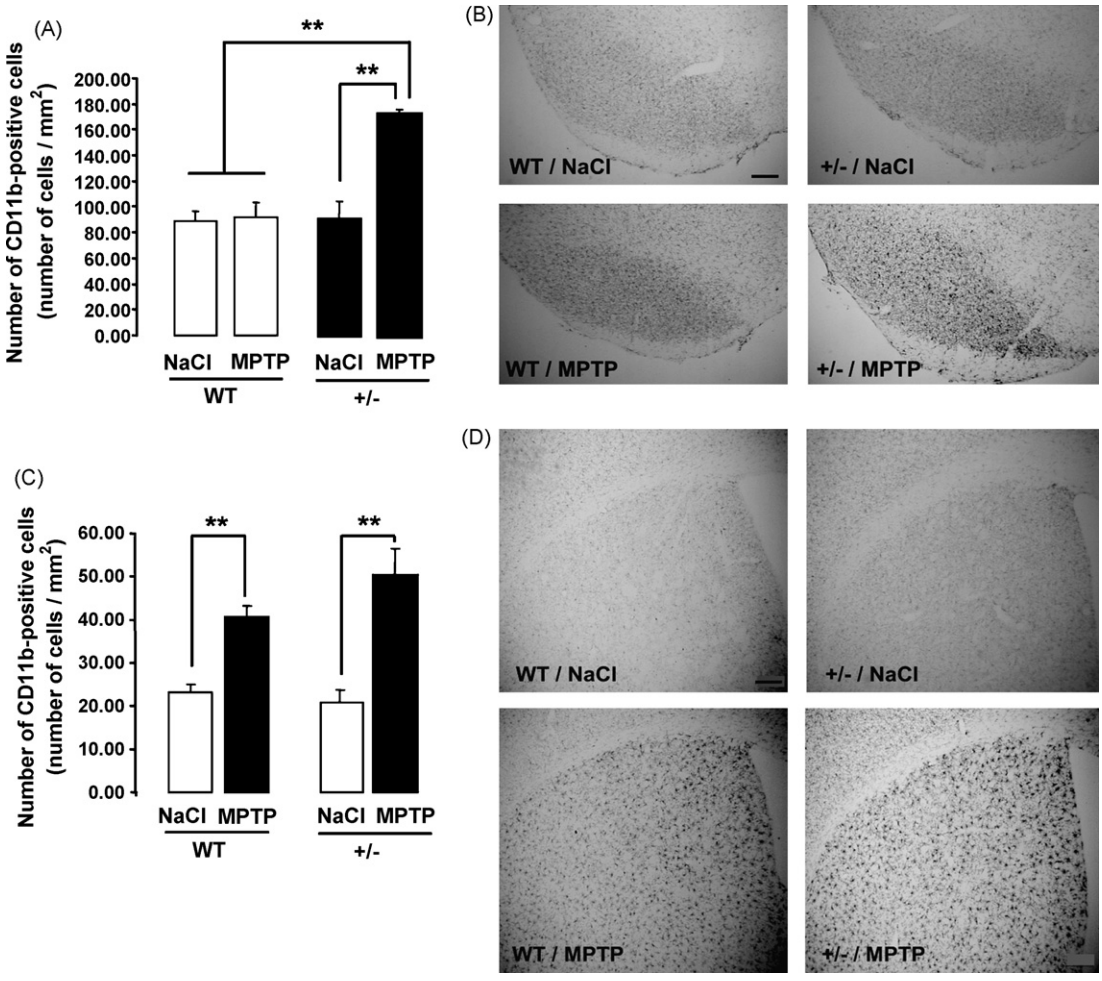

Fig. 3. Microglial activation is enhanced in IGF-1R$^{+/-}$ mice after MPTP treatment, compared to WT mice. (A and C) Quantification of CD11b-positive cells per μm^2 in the SN and striatum of WT and IGF-1R$^{+/-}$ mice after NaCl or MPTP treatment. ***$P < 0.001$ ($n = 5$ for WT/NaCl and WT/MPTP; $n = 3$ for +/−/NaCl and +/−/MPTP). Representative CD11b immunoreactivity is shown in the SN (B) and the striatum (D). Under control conditions, little staining is observed in the SN and the striatum of WT and IGF-1R$^{+/-}$ mice. MPTP treatment increases CD11b staining in IGF-1R$^{+/-}$ mice in the SN and in both WT and IGF-1R$^{+/-}$ mice in the striatum. Low magnification microphotographs: scale bar = 200 μm.

and Sawada, 2005) that participates in the cascade of events leading to neuronal degeneration. Moreover, IGF-1 is commonly assimilated to an anti-inflammatory cytokine, downregulating neuro-inflammatory processes. Consequently, considering the partial loss of IGF-1 functionality in heterozygous IGF-1R knockout mice, the latter might be more sensitive to neuro-inflammation than control mice, eventually leading to increased neuronal death. Therefore, microglial activation, the main marker of neuro-inflammation, was assessed before and after MPTP treatment in IGF-1R$^{+/-}$ and control mice. IGF-1R$^{+/-}$ mice displayed a significant 92% increase in microglial cell number in both SN pars compacta and reticulata (two-way ANOVA followed by *post hoc* Fisher's PLSD test; $P < 0.01$) compared to NaCl-treated IGF-1R$^{+/-}$ (Fig. 3A). Neuro-inflammatory processes also develop in the striatum, where dopaminergic terminals are degenerating. We therefore quantified CD11b-positive cells in that structure as well. The number of microglial cells was significantly higher after MPTP treatment both in WT and IGF-1R$^{+/-}$ mice (two-way ANOVA followed by *post hoc* Fisher's PLSD test; $P < 0.01$). However, even though increasing, the number of microglial cells was not statistically different after MPTP treatment in IGF-1R$^{+/-}$ mice compared to WT (Fig. 3C). Fig. 3B and D represents characteristic micrographs of CD11b staining in the SN (3B) and the striatum (3D) across all experimental conditions.

3.5. Genes associated with oxidative stress and anti-inflammatory action are downregulated in IGF-1R$^{+/-}$ mice

To compare above findings with a comprehensive display of gene expression we performed microarray analysis on IGF-1R$^{+/-}$ and WT mice. As MPTP toxicity involves a die back phenomenon starting in the striatum, we investigated the gene expression in the striatum. In this brain region, 128 genes were found to be significantly regulated in IGF-1R$^{+/-}$ compared to WT mice: inactivation of one IGF-1R allele resulted

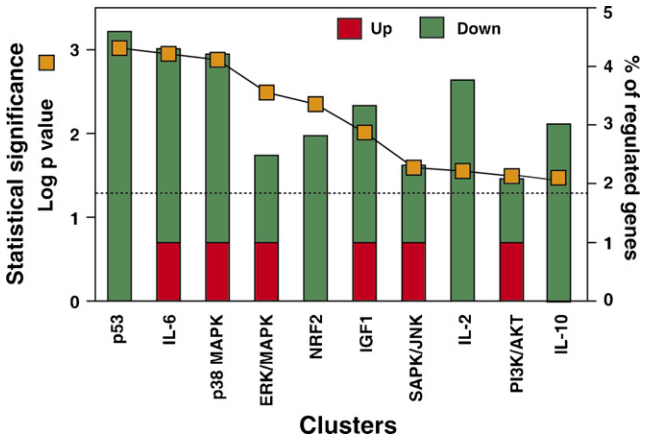

Fig. 4. Synthetic representation of gene expression changes in the striatum of IGF-1R$^{+/-}$ mice compared to WT. Relative clustering of significantly regulated genes into well-characterized signalling and metabolic pathways was determined by submitting the microarray dataset an ingenuity® pathway analysis. The relative number of regulated genes in each pathway (Bar graph/right *Y* axis) and the degrees of statistical significance for the involvement of each pathway (orange squares/left *Y* axis) are plotted. On the figure were conserved only canonical pathways with a *P*-value above the cut-off of 0.05 (indicated as a reference on the figure with a dotted line). For each pathway the relative proportion of gene found significantly downregulated appears in green whereas upregulated genes are depicted in red.

in a global pattern of gene downregulation (97 genes) in the striatum, while 31 genes showed significantly increased expression (supplementary figure). Remarkably, microarray analysis revealed that a major portion of regulated genes has been previously linked to cell death (Fig. 4). A number of downregulated genes are members of p53 and oxidative stress pathways, and several are functioning downstream of IGF-1R (Fig. 4). In particular, we observed a noticeable downregulation of the Akt and MAPkinase pathway, but not of the PI3K pathway (see supplementary data for details). Significantly, several gene families implicated in interleukin signalling were downregulated, such as IL-10 pathway that is capable of exerting anti-inflammatory action in a neuronal context. We hypothesize that this pattern of gene expression conditions the response of IGF-1R$^{+/-}$ mice to neurotoxins, in particular the overshooting inflammatory reaction that in turn may explain the increased damage in the brains of mutant individuals.

Interestingly, one of the genes found to be upregulated in IGF-1R$^{+/-}$ mice was the IGF-1R gene itself. While standard microarray analysis cannot distinguish between *WT* and *Igf1r*-null transcripts, previous studies revealed that in IGF-1R$^{+/-}$ mice both transcripts are present with similar relative abundance, indicating that the IGF-1R null-transcript is not destabilized, despite the disruption of receptor protein translation (Holzenberger et al., 2003). Given that IGF-1R$^{+/-}$ mice invariably display constitutive 50% decrease in IGF-1R protein level (Holzenberger et al., 2001), this suggests that both alleles upregulate *Igf1r* gene transcription in the brain, probably in an attempt to compensate for the loss-of-function mutation.

4. Discussion

Our main objective is to comprehend and further dissect the cellular mechanism behind the dual and antagonistic pro-oxidant and anti-inflammatory roles of IGF-1. Most inflammatory molecules, such as cytokines for instance, are double-edged molecules, either neuroprotective or neurotoxic, depending on the pathophysiological context. However, IGF-1 seems even more particular in the sense that its duality is expressed simultaneously in the same structure. While previous studies using cultured neurons suggested a neuroprotective action of IGF-1 in vitro, compatible with the here reported findings (Zhang et al., 1993; Offen et al., 2001), we here identified experimental conditions that highlight the duality of this growth factor and that might represent a model particularly useful for dissecting molecular events triggered by IGF-1. We used heterozygous IGF-1R$^{+/-}$ mice and submitted them to acute MPTP administration. Interestingly, MPTP induced more severe lesions in IGF-1R$^{+/-}$ mice than in wild-type control animals. We showed that both NO and ROS were decreased in IGF-1R$^{+/-}$ mice in comparison with controls, both before and after MPTP treatment. This was accompanied by a downregulation of oxidative stress-associated genes in the heterozygous knockout compared to WT mice. Furthermore, we found that IGF-1R$^{+/-}$ mice develop a dramatically increased neuro-inflammatory response in the substantia nigra, possibly related to interleukin signalling, that could well explain the increase in neuronal death. Interleukin gene expression pattern supported this interpretation. Unfortunately, we did not succeed in directly measuring interleukin levels in the different experimental conditions, probably due to the fact that we analyzed only 6 h posterior to the lesion (data not shown).

4.1. Neuro-inflammation induced by MPTP depends on IGF signalling

Neuro-inflammatory processes may participate in the cascade of events leading to neuronal degeneration induced by MPTP (Hirsch et al., 2005). Inhibition of these processes in MPTP-treated animals prevents neuronal degeneration. Even though still controversial, minocycline, an approved tetracycline derivative that inhibits microglial activation independently of its antimicrobial properties, has been shown to mitigate the demise of nigrostriatal dopaminergic neurons provoked by MPTP (Wu et al., 2002). Moreover, enhanced expression of TNF-α was associated with the earliest stages of damage in the MPTP model of dopaminergic neurotoxicity (Sriram et al., 2002; Pattarini et al., 2007). Accordingly, mice lacking receptors for TNF showed complete protection against MPTP-induced neurotoxicity (Sriram et al., 2002). Although those results are still debated, one cannot rule out a possible involvement of TNF-α in the mechanisms of cell death induced by MPTP intoxication (Rousselet et al., 2002). This is even more relevant here since IGF-1 is a potent inhibitor of TNF-α effects (Venters et al., 2000; Bluthe et

al., 2006; Palin et al., 2007; Ye et al., 2007). Thus TNF-α functionality is likely to be enhanced in IGF-1R$^{+/-}$ mice, which might lead to the increased neuronal death observed in our study.

4.2. IGF signalling has anti-inflammatory and pro-oxidative action in the brain

The classical view of microglial activity-induced neuronal death is that when overactivated, microglia can induce significant and highly detrimental neurotoxic effects by the excess production of a large array of cytotoxic factors such as superoxides (Colton and Gilbert, 1987), NO (Moss and Bates, 2001; Liu et al., 2002) and pro-inflammatory cytokines like TNF-α (Sawada et al., 1989; Lee et al., 1993). This was confirmed in the specific context of the SNc in which *in vitro* studies performed on neuron/glia mixed cultures showed that neuromelanin, a complex molecule that is released by dying dopaminergic neurons, was able to activate microglia (Zecca et al., 2003). In return, microglia phagocytosed and degraded neuromelanin together with the release of inflammatory factors (prostaglandins, cytokines) and ROS, which leads to neuronal death (Wilms et al., 2003). Remarkably, we found that both NO and ROS were decreased to the levels of the control (WT/NaCl) group in IGF-1R$^{+/-}$ mice, both before and after MPTP exposure, in substantia nigra, hippocampus and striatum. Thus, a conspicuous decrease of free radical production was unable to compensate for the loss of anti-inflammatory action accompanying the reduction of IGF-1 functionality. This means that even though NO/ROS production is likely to be the main feature by which microglia induces neuronal death, especially in the context of dopaminergic neurons (Block et al., 2007), in our context of partial IGF-1R inactivation, dopaminergic loss was independent of oxidative stress. Conversely, pro-inflammatory cascades have a greater impact on neurodegeneration, and IGF-1 is likely to be an important anti-inflammatory protagonist limiting neuronal death in MPTP-treated wild-type mice.

One possible explanation for such duality in IGF-1 function is a divergence in activation of intracellular signaling pathways. Binding of IGF-1 to its receptor promotes intrinsic tyrosine kinase activity that phosphorylates insulin receptor substrates (IRS-1 to -4) or Shc signal transduction molecules, which then leads to the activation of two main downstream signaling cascades, the MAPK and the phosphatidylinositol 3-kinase (PI3K) cascades (Guan, 1994; van der Geer et al., 1994; Melmed et al., 1996; Prisco et al., 1999). It is a widely held conception that clear separation of these two pathways is not possible, and that they are supposed to interact and, to a certain extent, replace each other (Burtscher and Christofori, 1999). However, our results show a clear dichotomy in IGF-1 action that would require a clear-cut functional compartmentalization of signaling pathways. Thus, either IGF-1, as an anti-inflammatory molecule, activates still unidentified signaling pathways, or the two known cascades are not cross-talking in the CNS. This latter possibility is supported by our microarray analysis, showing a downregulation of gene expression in Akt and MAPkinase pathways, but not in the PI3Kinase gene family. Clearly, these issues need more detailed exploration, particularly on the level of protein activation of the involved signalling cascades. Further studies are required to dissect the molecular events that open the way for oxidative and anti-inflammatory responses to IGF-1. This is even more important as it could lead to therapeutic strategies specifically targeting the pro-oxidant and not the anti-inflammatory intracellular signaling pathway.

Conflict of interest

There is no conflict of interest.

Acknowledgements

The University Victor Segalen, the CNRS, the Bordeaux Institute of Neuroscience (INSERM no. 8; CNRS no. 13) provided the infrastructural support for completion of the study.

Appendix A. Supplementary data

Supplementary data associated with this article can be found, in the online version, at doi:10.1016/j.neurobiolaging.2008.02.009.

References

Abercrombie, M., 1946. Estimation of nuclear population from microtome sections. Anat. Rec. 94, 239–247.

Berton, O., McClung, C.A., Dileone, R.J., Krishnan, V., Renthal, W., Russo, S.J., Graham, D., Tsankova, N.M., Bolanos, C.A., Rios, M., Monteggia, L.M., Self, D.W., Nestler, E.J., 2006. Essential role of BDNF in the mesolimbic dopamine pathway in social defeat stress. Science 311, 864–868.

Bezard, E., Dovero, S., Belin, D., Duconger, S., Jackson-Lewis, V., Przedborski, S., Piazza, P.V., Gross, C.E., Jaber, M, 2003. Enriched environment confers resistance to 1-methyl-4-phenyl-1,2,3,6-tetrahydropyridine and cocaine: involvement of dopamine transporter and trophic factors. J. Neurosci. 23, 10999–11007.

Bezard, E., Dovero, S., Imbert, C., Boraud, T., Gross, C.E., 2000. Spontaneous long-term compensatory dopaminergic sprouting in MPTP-treated mice. Synapse 38, 363–368.

Block, M.L., Zecca, L., Hong, J.S., 2007. Microglia-mediated neurotoxicity: uncovering the molecular mechanisms. Nat. Rev. Neurosci. 8, 57–69.

Blum, D., Torch, S., Lambeng, N., Nissou, M., Benabid, A.L., Sadoul, R., Verna, J.M., 2001. Molecular pathways involved in the neurotoxicity of 6-OHDA, dopamine and MPTP: contribution to the apoptotic theory in Parkinson's disease. Prog. Neurobiol. 65, 135–172.

Bluthe, R.M., Kelley, K.W., Dantzer, R., 2006. Effects of insulin-like growth factor-I on cytokine-induced sickness behavior in mice. Brain Behav. Immun. 20, 57–63.

Brouillet, E., Conde, F., Beal, M.F., Hantraye, P., 1999. Replicating Huntington's disease phenotype in experimental animals. Prog. Neurobiol. 59, 427–468.

Burtscher, I., Christofori, G., 1999. The IGF/IGF-1 receptor signaling pathway as a potential target for cancer therapy. Drug Resist Updat. 2, 3–8.
Cao, Y., Guo, P., Xu, Y., Zhao, B., 2005. Simultaneous detection of NO and ROS by ESR in biological systems. Methods Enzymol. 396, 77–83.
Colton, C.A., Gilbert, D.L., 1987. Production of superoxide anions by a CNS macrophage, the microglia. FEBS Lett. 223, 284–288.
D'Astous, M., Mendez, P., Morissette, M., Garcia-Segura, L.M., Di Paolo, T., 2006. Implication of the phosphatidylinositol-3 kinase/protein kinase B signaling pathway in the neuroprotective effect of estradiol in the striatum of 1-methyl-4-phenyl-1,2,3,6-tetrahydropyridine mice. Mol. Pharmacol. 69, 1492–1498.
Francis, J.W., Von Visger, J., Markelonis, G.J., Oh, T.H., 1995. Neuroglial responses to the dopaminergic neurotoxicant 1-methyl-4-phenyl-1,2,3,6-tetrahydropyridine in mouse striatum. Neurotoxicol. Teratol. 17, 7–12.
Gross, C.E., Ravenscroft, P., Dovero, S., Jaber, M., Bioulac, B., Bezard, E., 2003. Pattern of levodopa-induced striatal changes is different in normal and MPTP-lesioned mice. J. Neurochem. 84, 1246–1255.
Guan, K.L., 1994. The mitogen activated protein kinase signal transduction pathway: from the cell surface to the nucleus. Cell Signal 6, 581–589.
Guigoni, C., Dovero, S., Aubert, I., Qin, L., Bioulac, B.H., Bloch, B., Gurevich, E.V., Gross, C.E., Bezard, E., 2005. Levodopa-induced dyskinesia in MPTP-treated macaque is not dependent of the extent and pattern of the nigrostrial lesion. Eur. J. Neurosci. 22, 283–287.
Gundersen, H.J., Bendtsen, T.F., Korbo, L., Marcussen, N., Moller, A., Nielsen, K., Nyengaard, J.R., Pakkenberg, B., Sorensen, F.B., Vesterby, A., et al., 1988. Some new, simple and efficient stereological methods and their use in pathological research and diagnosis. Apmis 96, 379–394.
Hebert, G., Arsaut, J., Dantzer, R., Demotes-Mainard, J., 2003. Time-course of the expression of inflammatory cytokines and matrix metalloproteinases in the striatum and mesencephalon of mice injected with 1-methyl-4-phenyl-1,2,3,6-tetrahydropyridine, a dopaminergic neurotoxin. Neurosci. Lett. 349, 191–195.
Hirsch, E.C., Hunot, S., Hartmann, A., 2005. Neuroinflammatory processes in Parkinson's disease. Parkinsonism Relat. Disord. 11 Suppl. 1, S9–S15.
Holzenberger, M., Dupont, J., Ducos, B., Leneuve, P., Geloen, A., Even, P.C., Cervera, P., Le Bouc, Y., 2003. IGF-1 receptor regulates lifespan and resistance to oxidative stress in mice. Nature 421, 182–187.
Holzenberger, M., Hamard, G., Zaoui, R., Leneuve, P., Ducos, B., Beccavin, C., Perin, L., Le Bouc, Y., 2001. Experimental IGF-I receptor deficiency generates a sexually dimorphic pattern of organ-specific growth deficits in mice, affecting fat tissue in particular. Endocrinology 142, 4469–4478.
Jackson-Lewis, V., Jakowec, M., Burke, R.E., Przedborski, S., 1995. Time course and morphology of dopaminergic neuronal death caused by the neurotoxin 1-methyl-4-phenyl-1,2,3,6-tetrahydropyridine. Neurodegeneration 4, 257–269.
Kenchappa, P., Yadav, A., Singh, G., Nandana, S., Banerjee, K., 2004. Rescue of TNFalpha-inhibited neuronal cells by IGF-1 involves Akt and c-Jun N-terminal kinases. J. Neurosci. Res. 76, 466–474.
Kurkowska-Jastrzebska, I., Wronska, A., Kohutnicka, M., Czlonkowski, A., Czlonkowska, A., 1999. The inflammatory reaction following 1-methyl-4-phenyl-1,2,3,6-tetrahydropyridine intoxication in mouse. Exp. Neurol. 156, 50–61.
Lee, S.C., Liu, W., Dickson, D.W., Brosnan, C.F., Berman, J.W., 1993. Cytokine production by human fetal microglia and astrocytes. Differential induction by lipopolysaccharide and IL-1 beta. J. Immunol. 150, 2659–2667.
Liu, B., Gao, H.M., Wang, J.Y., Jeohn, G.H., Cooper, C.L., Hong, J.S., 2002. Role of nitric oxide in inflammation-mediated neurodegeneration. Ann. NY Acad. Sci. 962, 318–331.
MAQC-Consortium, 2006. The MicroArray Quality Control (MAQC) project shows inter- and intraplatform reproducibility of gene expression measurements. Nat. Biotechnol. 24, 1151–1161.
Melmed, S., Yamashita, S., Yamasaki, H., Fagin, J., Namba, H., Yamamoto, H., Weber, M., Morita, S., Webster, J., Prager, D., 1996. IGF-I receptor signalling: lessons from the somatotroph. Recent Prog. Horm. Res. 51, 189–215 (discussion 215–186).
Moss, D.W., Bates, T.E., 2001. Activation of murine microglial cell lines by lipopolysaccharide and interferon-gamma causes NO-mediated decreases in mitochondrial and cellular function. Eur. J. Neurosci. 13, 529–538.
Nagatsu, T., Sawada, M., 2005. Inflammatory process in Parkinson's disease: role for cytokines. Curr. Pharm. Des. 11, 999–1016.
Offen, D., Shtaif, B., Hadad, D., Weizman, A., Melamed, E., Gil-Ad, I., 2001. Protective effect of insulin-like-growth-factor-1 against dopamine-induced neurotoxicity in human and rodent neuronal cultures: possible implications for Parkinson's disease. Neurosci. Lett. 316, 129–132.
Palin, K., Bluthe, R.M., McCusker, R.H., Moos, F., Dantzer, R., Kelley, K.W., 2007. TNFalpha-induced sickness behavior in mice with functional 55 kDa TNF receptors is blocked by central IGF-I. J. Neuroimmunol. 187, 55–60.
Pattarini, R., Smeyne, R.J., Morgan, J.I., 2007. Temporal mRNA profiles of inflammatory mediators in the murine 1-methyl-4-phenyl-1,2,3,6-tetrahydropyrimidine model of Parkinson's disease. Neuroscience 145, 654–668.
Pera, J., Zawadzka, M., Kaminska, B., Szczudlik, A., 2004. Influence of chemical and ischemic preconditioning on cytokine expression after focal brain ischemia. J. Neurosci. Res. 78, 132–140.
Prisco, M., Romano, G., Peruzzi, F., Valentinis, B., Baserga, R., 1999. Insulin and IGF-I receptors signaling in protection from apoptosis. Horm. Metab. Res. 31, 80–89.
Reinhard Jr., J.F., Miller, D.B., O'Callaghan, J.P., 1988. The neurotoxicant MPTP (1-methyl-4-phenyl-1,2,3,6-tetrahydropyridine) increases glial fibrillary acidic protein and decreases dopamine levels of the mouse striatum: evidence for glial response to injury. Neurosci. Lett. 95, 246–251.
Rousselet, E., Callebert, J., Parain, K., Joubert, C., Hunot, S., Hartmann, A., Jacque, C., Perez-Diaz, F., Cohen-Salmon, C., Launay, J.M., Hirsch, E.C., 2002. Role of TNF-alpha receptors in mice intoxicated with the parkinsonian toxin MPTP. Exp. Neurol. 177, 183–192.
Russo, V.C., Gluckman, P.D., Feldman, E.L., Werther, G.A., 2005. The insulin-like growth factor system and its pleiotropic functions in brain. Endocr. Rev. 26, 916–943.
Ryu, J.K., Nagai, A., Kim, J., Lee, M.C., McLarnon, J.G., Kim, S.U., 2003. Microglial activation and cell death induced by the mitochondrial toxin 3-nitropropionic acid: in vitro and in vivo studies. Neurobiol. Dis. 12, 121–132.
Sawada, M., Kondo, N., Suzumura, A., Marunouchi, T., 1989. Production of tumor necrosis factor-alpha by microglia and astrocytes in culture. Brain Res. 491, 394–397.
Shen, J.G., Quo, X.S., Jiang, B., Li, M., Xin, W., Zhao, B.L., 2000. Chinonin, a novel drug against cardiomyocyte apoptosis induced by hypoxia and reoxygenation. Biochim. Biophys. Acta 1500, 217–226.
Sriram, K., Matheson, J.M., Benkovic, S.A., Miller, D.B., Luster, M.I., O'Callaghan, J.P., 2002. Mice deficient in TNF receptors are protected against dopaminergic neurotoxicity: implications for Parkinson's disease. FASEB J. 16, 1474–1476.
Theoret, H., Boire, D., Herbin, M., Ptito, M., 1999. Stereological evaluation of substantia nigra cell number in normal and hemispherectomized monkeys. Brain Res. 835, 354–359.
Tunez, I., Montilla, P., Del Carmen Munoz, M., Feijoo, M., Salcedo, M., 2004. Protective effect of melatonin on 3-nitropropionic acid-induced oxidative stress in synaptosomes in an animal model of Huntington's disease. J. Pineal Res. 37, 252–256.
van der Geer, P., Hunter, T., Lindberg, R.A., 1994. Receptor protein-tyrosine kinases and their signal transduction pathways. Annu. Rev. Cell Biol. 10, 251–337.
Venters, H.D., Dantzer, R., Kelley, K.W., 2000. Tumor necrosis factor-alpha induces neuronal death by silencing survival signals generated by the type I insulin-like growth factor receptor. Ann. NY Acad. Sci. 917, 210–220.
Venters, H.D., Tang, Q., Liu, Q., VanHoy, R.W., Dantzer, R., Kelley, K.W., 1999. A new mechanism of neurodegeneration: a proinflammatory cytokine inhibits receptor signaling by a survival peptide. Proc. Natl. Acad. Sci. U.S.A. 96, 9879–9884.

Wang, J., Green, P.S., Simpkins, J.W., 2001. Estradiol protects against ATP depletion, mitochondrial membrane potential decline and the generation of reactive oxygen species induced by 3-nitroproprionic acid in SK-N-SH human neuroblastoma cells. J. Neurochem. 77, 804–811.

Watanabe, Y., Himeda, T., Araki, T., 2005. Mechanisms of MPTP toxicity and their implications for therapy of Parkinson's disease. Med. Sci. Monit. 11, RA17–RA23.

West, M.J., Gundersen, H.J., 1990. Unbiased stereological estimation of the number of neurons in the human hippocampus. J. Comp. Neurol. 296, 1–22.

Wilms, H., Rosenstiel, P., Sievers, J., Deuschl, G., Zecca, L., Lucius, R., 2003. Activation of microglia by human neuromelanin is NF-kappaB dependent and involves p38 mitogen-activated protein kinase: implications for Parkinson's disease. FASEB J. 17, 500–502.

Wu, D.C., Jackson-Lewis, V., Vila, M., Tieu, K., Teismann, P., Vadseth, C., Choi, D.K., Ischiropoulos, H., Przedborski, S., 2002. Blockade of microglial activation is neuroprotective in the 1-methyl-4-phenyl-1,2,3,6-tetrahydropyridine mouse model of Parkinson disease. J. Neurosci. 22, 1763–1771.

Ye, P., Kollias, G., D'Ercole, A.J., 2007. Insulin-like growth factor-I ameliorates demyelination induced by tumor necrosis factor-alpha in transgenic mice. J. Neurosci. Res. 85, 712–722.

Ye, P., Price, W., Kassiotis, G., Kollias, G., D'Ercole, A.J., 2003. Tumor necrosis factor-alpha regulation of insulin-like growth factor-I, type 1 IGF receptor, and IGF binding protein expression in cerebellum of transgenic mice. J. Neurosci. Res. 71, 721–731.

Zecca, L., Zucca, F.A., Wilms, H., Sulzer, D., 2003. Neuromelanin of the substantia nigra: a neuronal black hole with protective and toxic characteristics. Trends Neurosci. 26, 578–580.

Zhang, Y., Tatsuno, T., Carney, J.M., Mattson, M.P., 1993. Basic FGF, NGF, and IGFs protect hippocampal and cortical neurons against iron-induced degeneration. J. Cereb. Blood Flow Metab. 13, 378–388.